Acta Crystallographica Section A
Foundations of Crystallography
ISSN 0108-7673

Received 11 February 2000
Accepted 20 June 2000

Anharmonicity in anisotropic displacement parameters

H. B. Bürgi,[a]* S. C. Capelli[a] and H. Birkedal[b]

[a]Laboratorium für Kristallographie der Universität Bern, Freiestrasse 3, CH-3012 Bern, Switzerland, and [b]Institut de Cristallographie, Université de Lausanne, BSP-Dorigny, CH-1015 Lausanne, Switzerland. Correspondence e-mail: hans-beat.buergi@krist.unibe.ch

A quasi-harmonic molecular-mean-field model for analyzing anharmonic temperature evolution of anisotropic displacement parameters is described. Anharmonic effects are taken into account through a Grüneisen-type temperature dependence of effective vibrational frequencies. The method is applied to neutron and X-ray diffraction data of hexamethylenetetramine measured between 15 and 298 K. The resulting Grüneisen parameters and other characteristics of molecular motion in the solid state agree well with those obtained from independent vibrational data. The analysis also suggests errors in the ADP's due to insufficient extinction corrections in the diffraction data.

1. Introduction

Diffraction experiments with neutrons or X-rays yield information on the scattering density in a crystal averaged over space and time. This information is usually parameterized in terms of spherically symmetric atomic form factors and Gaussian distribution functions to obtain mean atomic positions and harmonic displacement parameters. When the measurements are sufficiently accurate, additional information on chemical bonding and anharmonic thermal vibrations can be extracted from the structure amplitudes. Multipolar deformation functions (Stewart, 1976; Coppens, 1997) and Gram–Charlier series expansions of probability density functions (Johnson & Levy, 1974; Coppens, 1993) are often used in structure refinement to account, respectively, for asphericity of form factors and deviation from Gaussian distributions. These parameterizations have the advantage of providing a general and potentially complete model of the electron density at the level of the independent-atom approximation to the electron-density function. Their disadvantage is that the number of parameters increases sharply with the order of the multipolar or Gram–Charlier expansion. These models do not account explicitly for the temperature dependence of the probability density function but their parameters, determined at different temperatures, may be tested *a posteriori* for the expected dependence (*e.g.* T^0 for multipolar parameters, T for anisotropic displacement parameters, T^2 for third-order anharmonicity parameters *etc.*)

Here we present an alternative relatively simple method to parameterize effects of anharmonicity in diffraction data. It is based on a recently developed model for analyzing the temperature evolution of anisotropic displacement parameters (ADP's), *i.e.* of the central second moments of the atomic probability density function (Bürgi & Förtsch, 1999; Bürgi & Capelli, 2000; Capelli *et al.*, 2000). The model assumes a harmonic molecular mean field and considers temperature-dependent as well as temperature-independent contributions to ADP's. The former account for low-frequency normal modes of vibration and are characterized by effective frequencies and associated atomic displacement vectors. The latter account for the high-frequency normal modes and take the form of an atom-specific correction term. At high temperatures, it is sometimes observed that ADP's do not increase linearly with temperature, *i.e.* they do not show harmonic behavior. Such effects can largely be taken into account through a simple Grüneisen-type temperature dependence of the frequency of each normal mode (Grüneisen, 1926), together with the assumption that the associated eigenvectors do not change. The anharmonic model has the same form as the harmonic one and is sometimes called the quasi-harmonic model.

This approach is illustrated with an analysis of the ADP's of hexamethylenetetramine (HMT) studied by neutron and X-ray diffraction at seven different temperatures [15, 50, 80, 120, 160, 200 and 298 K (Dickinson & Raymond, 1923; Duckworth *et al.*, 1970; Stevens & Hope, 1975; Kampermann *et al.*, 1994, 1995; Terpstra *et al.*, 1995)]. Effects of anharmonicity on effective vibrational frequencies are compared to those observed directly by neutron inelastic scattering (Dolling & Powell, 1970; Thomas & Ghosh, 1975). Results obtained by vibrational spectroscopy (Bertie & Solinas, 1974; Cyvin, 1972) and specific heat measurements will also be considered (Chang & Westrum, 1960). This work shows that the simple quasi-harmonic model can quantify, through a Grüneisen parameter, the anharmonic motion of the HMT molecules in the solid state. An analysis based on a simpler model was presented earlier (Birkedal *et al.*, 1997).

2. ADP analysis

In the harmonic approximation, the mean-square displacement $\langle u^2 \rangle$ of a quantum oscillator from its equilibrium position is given by

$$\langle u^2 \rangle = \hbar/(2\omega m)\coth[\hbar\omega/(2k_BT)], \quad (1)$$

where m is the mass of the oscillator, ω the vibrational frequency, $\hbar$ the Planck constant ($\hbar = h/2\pi$), k_B the Boltzmann constant and T the temperature (Cyvin, 1968). Fig. 1 shows the temperature dependence of $\langle u^2 \rangle$. In the low-temperature limit, $\langle u^2 \rangle$ is inversely proportional to ω and independent of T:

$$\langle u^2 \rangle = \hbar/(2\omega m) = \delta_0 \quad (T \rightarrow 0), \quad (2)$$

where δ_0 represents the zero-point mean-square amplitude (quantum regime). In the high-temperature limit, $\langle u^2 \rangle$ behaves classically; it varies linearly with the temperature and with the inverse square of ω:

$$\langle u^2 \rangle = k_BT/(\omega^2 m) = sT \quad (T \rightarrow \infty), \quad (3)$$

where s is the slope of the curve in the linear region. This relation also implies that mean-square amplitudes measured at high temperature must extrapolate to zero at 0 K. Whenever experimentally determined ADP's do not fulfil this condition, additional factors contribute to the ADP's, *e.g.* anharmonicity, vibrations with large frequencies, disorder or systematic error.

At temperature Θ'_E, the zero-point mean-square amplitude and the classical mean-square amplitude are the same:

$$\Theta'_E = \hbar\omega/(2k_B) = \Theta_E/2. \quad (4)$$

Θ'_E is half of the Einstein temperature Θ_E. It can be considered the borderline between the two limiting regimes.

In the molecular mean-field approximation, the motions of a molecule in a crystal are modeled with a collection of independent oscillators moving in an effective potential given by the average crystal environment (Bürgi, 1995). This leads to a simple description of the temperature evolution of the ADP's. The physical and mathematical details are given elsewhere (Förtsch, 1997; Bürgi & Förtsch, 1999; Bürgi & Capelli, 2000). Here we recall only the general expression

$$\mathbf{\Sigma}^x = \mathbf{AgV}\boldsymbol{\delta}(\omega, T)\mathbf{V}^T\mathbf{g}^T\mathbf{A}^T + \boldsymbol{\varepsilon}^x. \quad (5)$$

$\mathbf{\Sigma}^x$ is the mean-square amplitude matrix in atomic positional coordinates. The 3×3 diagonal blocks of the $\mathbf{\Sigma}^x$ matrix are the ADP's obtainable from elastic diffraction experiments. The off-diagonal blocks are not available from such experiments, implying that the direct information on the coupling of atomic motions is lost. The matrix $\boldsymbol{\delta}$ is diagonal with elements $\delta_j = \hbar/(2\omega_j)\coth[\hbar\omega_j/(2k_BT)]$; the δ_j's are the temperature-dependent mean-square amplitudes of the low-frequency molecular vibrations, mainly translation and libration. The matrix $\mathbf{V}$ transforms normal coordinates to mass-adjusted molecular coordinates. The product matrix (**Ag**) represents the transformation from mass-adjusted molecular coordinates to atomic positional coordinates and depends only on atomic coordinates and masses. The correction term $\boldsymbol{\varepsilon}^x$ accounts for temperature-independent contributions such as those from high-frequency molecular vibrations and disorder but also those due to inadequate treatment of absorption, extinction, valence electron density *etc.* The different contributions to $\boldsymbol{\varepsilon}^x$ can be separated reliably only with the help of additional independent information and empirical rules derived from IR and Raman spectroscopy or *ab initio* calculations of vibrational properties (Higgs, 1955). Empirically, it is found that the values of $\boldsymbol{\varepsilon}^x$ derived from the ADP's are in good agreement with the ones calculated from spectroscopic data (Förtsch, 1997) if disorder, anharmonicity and systematic errors in the diffraction data or in the model are negligible (Capelli, 1999). In practice, $\boldsymbol{\varepsilon}^x$ is expressed through individual $\boldsymbol{\varepsilon}$ tensors defined in a local coordinate system for each atom and transformed to the working coordinate system by $\boldsymbol{\varepsilon}^x = \mathbf{T}\boldsymbol{\varepsilon}\mathbf{T}^T$. This allows the same $\boldsymbol{\varepsilon}$ to be assigned to symmetrically equivalent or chemically similar atoms in a molecule.

The lack of information on the off-diagonal 3×3 blocks of the mean-square amplitude matrix $\mathbf{\Sigma}^x$ can be compensated, to some extent, by measuring the diagonal part of $\mathbf{\Sigma}^x$ at multiple temperatures. From such data, the unknowns in equation (5), namely the elements of the eigenvector matrix $\mathbf{V}$, the normal frequencies ω_j and the diagonal 3×3 blocks $\boldsymbol{\varepsilon}$ of $\boldsymbol{\varepsilon}^x$ can be determined *via* a non-linear least-squares procedure after expansion in a Taylor series to first order. The full calculation

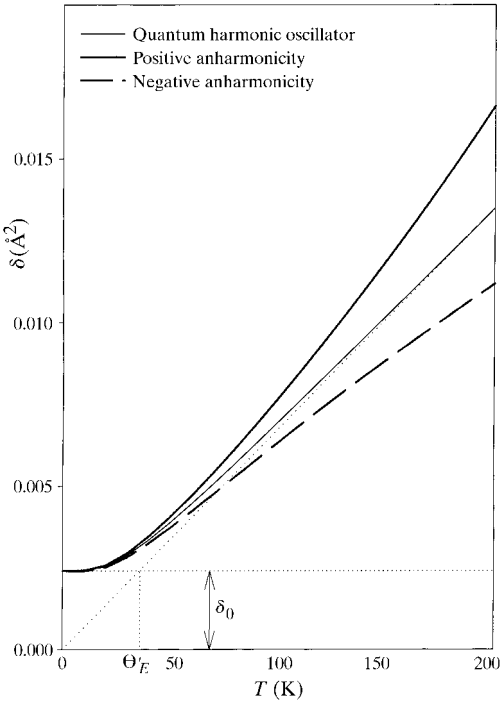

Figure 1
Temperature dependence of the mean-square amplitude of a single oscillator. Comparison between harmonic (thin solid line), positive anharmonic (thick solid line) and negative anharmonic (dashed thick line) mean-square displacements as calculated using equation (1), where the expression for the frequency is that given in equation (18) and the numerical values are: $\omega = 50$ cm^{-1}, $m = 140$ a.m.u., $\chi = 2 \times 10^{-4}$ and $\gamma_G = 0.0$, 2.5 and -2.5, respectively. The zero-point mean-square amplitude δ_0 (double arrow), the linearity of the harmonic curve at high temperature and the characteristic temperature Θ'_E are also shown (dotted lines).

is implemented in a computer program (Förtsch, 1997; Capelli, 1999). A simple extension of this analysis capable of dealing with the main effects of anharmonicity is discussed in the next section.

3. Anharmonicity

The model outlined above is harmonic but real crystals are anharmonic: they commonly expand on heating. On average, the interactions between the atoms are thereby reduced, leading to a reduction of the vibration frequencies and to mean-square amplitudes of motion that are larger than expected for a harmonic crystal (positive anharmonicity). It is also possible that a crystal shrinks on heating and therefore the vibration frequencies increase while the mean-square amplitudes decrease with respect to harmonic behavior (negative anharmonicity; Evans *et al.*, 1997). In Fig. 1, the mean-square displacements of anharmonic oscillators are compared to those of a harmonic one. Linear extrapolation of the high-temperature part of the anharmonic curves ($T > 2\Theta'_E$) no longer implies zero mean-square amplitudes at 0 K, but negative values in the case of positive anharmonicity and positive values in the case of negative anharmonicity. If a harmonic analysis of ADP's leads to physically impossible, negative or implausibly large positive $\boldsymbol{\varepsilon}^x$ tensors, anharmonic motion is indicated.

A description of such motion is developed on the basis of the classical and quantum-mechanical monoatomic linear chains with nearest-neighbor interactions. The treatment is then generalized to the three-dimensional crystal and incorporated into the model of ADP analysis summarized in the preceding section. N identical atoms with mass m arranged in a regular chain are assumed to interact through a generic anharmonic potential V, *e.g.* a Morse potential (Fig. 2; Morse, 1929), a Lennard-Jones (12,6) potential (Lennard-Jones, 1924) or a Buckingham (exp,6) potential (Buckingham, 1938). For our purposes, the specific form of the empirical parameterization is unimportant, since the sum of repulsive and dispersive interatomic interactions will be replaced by a polynomial expansion.

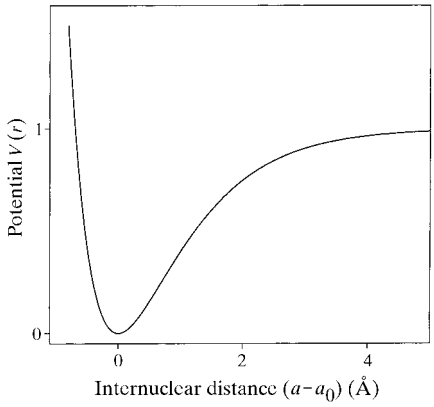

Figure 2
Representation of the anharmonic Morse potential as function of the interatomic distance $(a - a_0)$.

If the average interatomic distance $a(T)$ changes with increasing temperature, it is convenient to express the potential energy of the chain as a function of this change $\Delta a(T) = a(T) - a_0$, where a_0 is the equilibrium interatomic spacing. The potential energy of the chain, represented as a Taylor expansion, is, to within an additive constant,

$$\begin{aligned} V(T) = f_0 \sum_l [\Delta a(T) + u_l - u_{l+1}]^2/2 \\ + g_0 \sum_l [\Delta a(T) + u_l - u_{l+1}]^3/3! \\ + h_0 \sum_l [\Delta a(T) + u_l - u_{l+1}]^4/4! + \ldots \end{aligned} \quad (6)$$

with u_l the instantaneous displacement of the lth atom in the chain from its mean separation $a_0 + \Delta a(T)$ and u_{l+1} the instantaneous displacement of its adjacent neighbor; f_0, g_0 and h_0 are, respectively, the quadratic, cubic and quartic force constants of the potential-energy function.

The equilibrium probability density function

$$P(u_1, u_2, \ldots, u_N) = \frac{\exp[-V(\Delta a(T), u_1, u_2, \ldots, u_N)/k_b T]}{\int_{-\infty}^{+\infty} \exp[-V(\Delta a(T), u_1, u_2, \ldots, u_N)/k_b T]\, \mathrm{d}u_1\, \mathrm{d}u_2 \ldots \mathrm{d}u_N} \quad (7)$$

minimizes the potential-energy contribution to the Helmholtz free energy F of the chain.

$$\begin{aligned} F(P) = \int_{-\infty}^{+\infty} P(u_1, u_2, \ldots, u_N) V(u_1, u_2, \ldots, u_N)\, \mathrm{d}u_1\, \mathrm{d}u_2 \ldots \mathrm{d}u_N \\ + k_B T \int_{-\infty}^{+\infty} P(u_1, u_2, \ldots, u_N) \\ \times \ln P(u_1, u_2, \ldots, u_N)\, \mathrm{d}u_1\, \mathrm{d}u_2 \ldots \mathrm{d}u_N, \end{aligned} \quad (8)$$

where the first term represents the internal energy and the second term the entropy contribution. In line with the mean-field model introduced in the previous section, the equilibrium density function is approximated by a product of independent harmonic oscillator probability densities, one for each atom (Thomas, 1971):

$$P'(u_1, u_2, \ldots, u_N) = 1/(2\pi\sigma)^{N/2} \prod_{l=1}^{N} \exp(-u_l^2/2\sigma). \quad (9)$$

The atomic probability density function of each atom is a Gaussian with width $\sigma(T)^{1/2}$ and centered at the mean atomic position, *i.e.* two consecutive Gaussians are a distance $a(T)$ apart. Recall that

$$\begin{aligned} \langle u_l^n \rangle &= 1/(2\pi\sigma)^{1/2} \int_{-\infty}^{+\infty} u_l^n \exp(-u_l^2/2\sigma)\, \mathrm{d}u_l \\ &= \begin{cases} 0 & \text{for } n \text{ odd} \\ 1 \times 3 \times \ldots \times (n-1)\sigma^{n/2} & \text{for } n \text{ even} \end{cases} \end{aligned} \quad (10)$$

so the free energy becomes

$$F(P') = f_0\Delta a(T)^2/2 + g_0\Delta a(T)^3/3! + h_0\Delta a(T)^4/4! + [f_0 + g_0\Delta a(T) + h_0\Delta a(T)^2/2]\sigma + h_0\sigma^2/2 - (k_BT/2)\ln\sigma. \quad (11)$$

The first three terms represent the thermal elastic energy. The terms linear in σ represent the quasi-harmonic energy, so called because the expression in square brackets looks like an effective harmonic force constant f, albeit one that depends on thermal expansion Δa and thus on temperature. The quartic anharmonic contribution to the energy is given by $h_0\sigma^2/2$ and the entropic contribution by $(k_BT/2)\ln\sigma$. Except for a small difference in the quartic anharmonic energy, this result is the same as that of a more complete lattice dynamical treatment (Brüesch, 1982).

Since the trial probability density function P' is only approximate, $F(P')$ must be minimized by optimizing Δa and σ with the so-called mean field relations

$$\partial F(P')/\partial\sigma = f\sigma + h_0\sigma^2 - k_BT/2 = 0 \quad (12)$$

$$\partial F(P')/\partial\Delta a = f_0\Delta a(T) + g_0\Delta a(T)^2/2 + h_0\Delta a(T)^3/6 + [g_0 + h_0\Delta a(T)]\sigma = 0. \quad (13)$$

For a classical oscillator, it follows from the first condition that

$$\sigma(T) \cong k_BT/2f(T) = k_BT/[2m\omega_{\rm eff}^2(T)], \quad (14)$$

if second- and higher-order terms in T/f are neglected. This looks like the mean-square amplitude of a harmonic oscillator, but with temperature-dependent force constant f or vibrational frequency $\omega_{\rm eff}$. For a quantum oscillator,

$$\sigma(T) \cong \hbar/[2m\omega_{\rm eff}(T)]\coth[\hbar\omega_{\rm eff}(T)/(2k_BT)]. \quad (15)$$

From the second condition, an upper limit for Δa is obtained,

$$\Delta a(T) \cong -g_0k_BT/2f_0^2, \quad (16)$$

if terms in h_0 are neglected. Note that for the quantum oscillator the average interatomic distance at 0 K, $a(0)$, differs from the equilibrium separation a_0. It can be obtained by numerical solution of the second mean-field relation [equation (13)].

The explicit expression for the effective frequency $\omega_{\rm eff}$ becomes

$$\omega_{\rm eff} \cong (f_0/m)^{1/2}[1 - g_0^2k_BT/4f_0^3] = \omega_0\{1 + (a_0g_0/2f_0)[\Delta a(T)/a_0]\}, \quad (17)$$

where $\omega_0 = (f_0/m)^{1/2}$ is the corresponding harmonic frequency. The relative change in frequency is thus proportional to the thermal expansion χT (Brüesch, 1982) and to a proportionality factor called the Grüneisen parameter γ_G (Grüneisen, 1926):

$$\Delta\omega/\omega_0 = -\gamma_G\chi T, \quad (18)$$

where $\gamma_G = -a_0g_0/2f_0$ and χ is the thermal expansion coefficient. This approximation can be transferred to the three-dimensional crystal. Grüneisen parameters are defined in analogy to equation (18):

$$\Delta\omega(j)/\omega_0(j) = -\gamma_G(j)\Delta V(T)/V_0 = -\gamma_G(j)\chi T, \quad (19)$$

Table 1
Ab initio equilibrium geometry compared with the 15 K neutron data from Kampermann *et al.* (1995).

Coordinates (Å)		Interatomic parameters		
Present work			Present work	From Kampermann *et al.* (1995)
x(C)	1.67343	C—H (Å)	1.084	1.097 (3)
x(H)	2.31121	C—N (Å)	1.460	1.473 (2)
y(H)	−0.61969	N—C—H (°)	109.24	108.4 (2)
x(N)	0.85561	H—C—H (°)	107.91	110.7 (2)
		N—C—N (°)	111.89	112.6 (5)
		C—N—C (°)	108.23	108.0 (1)

one for every normal mode j considered explicitly in equation (5). The unit-cell volume V_0 at 0 K is usually not available. Therefore, the expression $\Delta V(T)/V_0$ is replaced by $\Delta V(T)/V_{\rm min}$, where $V_{\rm min}$ is the unit-cell volume at the lowest experimental temperature $T_{\rm min}$. The volume $V(T)$ is expressed as a power series in the temperature, $V(T) = V_0 + v_1T + v_2T^2 + \ldots$; the coefficients v_1, v_2 of thermal expansion are obtained by linear regression. With the difference $\Delta V(T) = V(T) - V_0$, which is independent of V_0, the expression for the frequencies used in numerical calculations becomes

$$\omega_{\rm eff}(j, T) = \omega_0(j)[1 - \gamma_G(j)\Delta V(T)/V_{\rm min}], \quad (20)$$

where $\omega_{\rm eff}$ is the effective anharmonic frequency of the normal mode j at temperature T and ω_0 is the corresponding harmonic frequency. The atomic mean-square amplitudes are

$$\mathbf{\Sigma}^x = \mathbf{AgV}\boldsymbol{\delta}(\omega_0, T, \gamma_G)\mathbf{V}^T\mathbf{g}^T\mathbf{A}^T + \boldsymbol{\varepsilon}^x, \quad (21)$$

where $\boldsymbol{\delta}$ is now also a function of the Grüneisen parameters γ_G. As before, γ_G depends on the higher-order force constants considered in the series expansion of the interatomic potential. Note that this approximation assumes that the eigenvectors $\mathbf{V}$ do not change under the influence of anharmonicity. This approximation may not always hold at very high temperatures. Except for the dependence of $\boldsymbol{\delta}$ on γ_G, the anharmonic model in equation (21) looks the same as the harmonic one in equation (15), and is therefore called 'quasi-harmonic' (Willis & Pryor, 1975).

4. Application to hexamethylenetetramine

Hexamethylenetetramine (HMT) has attracted interest from the chemistry and physics communities for a long time because its molecular structure is simple and its molecular symmetry is high ($\bar{4}3m$). The latter is preserved in the solid state, since the molecule occupies special positions with the same symmetry in space group $I\bar{4}3m$. The asymmetric unit is composed of only three atoms, all of them sitting in special positions (Table 1). Several diffraction investigations have been reported for HMT: the pioneering X-ray study at several temperatures by Becka & Cruickshank (1963); highly accurate neutron measurements, corrected for absorption, extinction and

thermal diffuse scattering (Duckworth *et al.*, 1970) and high-resolution X-ray measurements, corrected for thermal diffuse scattering (Stevens & Hope, 1975), both of them taken at 298 K and re-refined with third-order Gram–Charlier coefficients for the description of anharmonic vibrations (Terpstra *et al.*, 1995); X-ray diffraction measurements at 120 K used for charge-density studies (Kampermann *et al.*, 1994); more recent neutron diffraction measurements at 15, 50, 80, 120, 160, 200 K undertaken to study the effects of extinction and nuclear thermal vibrations (Kampermann *et al.*, 1995). The latter data represent a consistent set of measurements performed on the same crystal and processed with the same techniques. Their precision decreases somewhat with increasing temperature: between 15 and 200 K; the standard deviations $\sigma(U^{ij})$ vary from 0.0002 to 0.0006 Å^2 for C and N, and from 0.0004 to 0.0011 Å^2 for H (Kampermann *et al.*, 1995). Related data from different techniques are also available: mean-square amplitudes for the hydrogen atoms from incoherent neutron inelastic scattering (Thomas & Ghosh, 1975) and from vibrational analysis (Cyvin, 1972), experimental IR and Raman frequencies (Bertie & Solinas, 1974), phonon-dispersion curves at 100 and 298 K from coherent neutron inelastic scattering on deuterated HMT (DHMT; Dolling & Powell, 1970), as well as specific heat data (Chang & Westrum, 1960).

In order to test the method of analysis outlined in the two preceding sections and the potential of the quasi-harmonic approximation implemented in it, the ADP's of HMT measured by neutron diffraction experiments at 15, 50, 80, 120, 160 and 200 K are studied first (Kampermann *et al.*, 1995). The best model of motion obtained from these data (54 ADP's) is then refined against all nine available sets of accurate structural data (81 ADP's) to test model robustness. The results are compared to the independent non-diffraction information.

The model of motion consists of the six low-frequency external modes of vibration and of three temperature-independent correction terms ε, one each for N, C and H. Because of the cubic site symmetry, the three translation frequencies are degenerate, as are the three librational frequencies. Thus, there are only two independent frequencies with corresponding Grüneisen parameters to be determined. Libration and translation belong to two different irreducible representations of the molecular point group (T_1 and T_2, respectively); therefore, they do not mix and the 6×6 eigenvector matrix **V** is simply a unit matrix.

The coordinate system used in the analysis is Cartesian. Its axes coincide with the crystallographic $\bar{4}$ axes, *i.e.* they pass through pairs of carbon atoms. The local coordinate system for the nitrogen atom has the x direction along the threefold axis; the y direction is orthogonal to the threefold axis in one of the molecular mirror planes and the z direction is orthogonal to the previous two. The site symmetry of the nitrogen atom is $3m$, implying the constraints $\varepsilon_{ij} = 0$ for $i \neq j$ and $\varepsilon_{22} = \varepsilon_{33}$ (1 stands for the x, 2 for the y and 3 for the z direction). The local coordinate system of the carbon atom has its x axis along the $\bar{4}$ axis, the y axis in the mirror plane containing the neighboring nitrogen atoms and the z axis in the mirror plane containing the bonded hydrogen atoms. The site symmetry is $mm2$ so that $\varepsilon_{ij} = 0$ for $i \neq j$. The local coordinate system for the hydrogen atom is defined with x along the C—H bond, y parallel to the mirror plane containing the nitrogen atoms and z in the H—C—H plane, orthogonal to the previous two; the site symmetry is m so that ε_{13} may differ from zero. Each of the local coordinate systems is right-handed Cartesian.

Visual inspection of the ADP's plotted as a function of temperature (Fig. 3) shows that, except for U^{11} of the hydrogen atoms, the mean-square amplitudes at temperatures larger than 100 K extrapolate to more or less negative values at 0 K. This, together with the thermal expansion of the crystal lattice, is a clear indication of anharmonicity [$a(15\,\text{K}) = 6.9274\,(8)$, $a(298\,\text{K}) = 7.028\,(2)$ Å].

Numerical calculations are based on the model given in equation (21). The parameters optimized in each model are listed in Table 2. The results for the harmonic model 1_h confirm the visual impression (Table 2). The elements of $\boldsymbol{\varepsilon}$(C) and $\boldsymbol{\varepsilon}$(N) are negative, *i.e.* unphysical, and those of $\boldsymbol{\varepsilon}$(H) are too small compared to those calculated *ab initio* (see below, Table 3). Although the agreement factor ($wR2$ ~3%) and the goodness of fit (~1.4) look quite impressive, the differences ($\mathbf{U}_{\text{obs}} - \mathbf{U}_{\text{calc}}$) plotted in Fig. 4(*a*) tell a different story. A systematic trend can be recognized: differences are overwhelmingly positive at 15, 160 and 200 K and negative at the three intermediate temperatures. Both observations indicate the presence of anharmonicity.

Several anharmonic models have been tried. Introducing a Grüneisen constant for either translation or libration (Table 2, models 1_at, 1_al), the components of $\boldsymbol{\varepsilon}$(N) and $\boldsymbol{\varepsilon}$(C) become

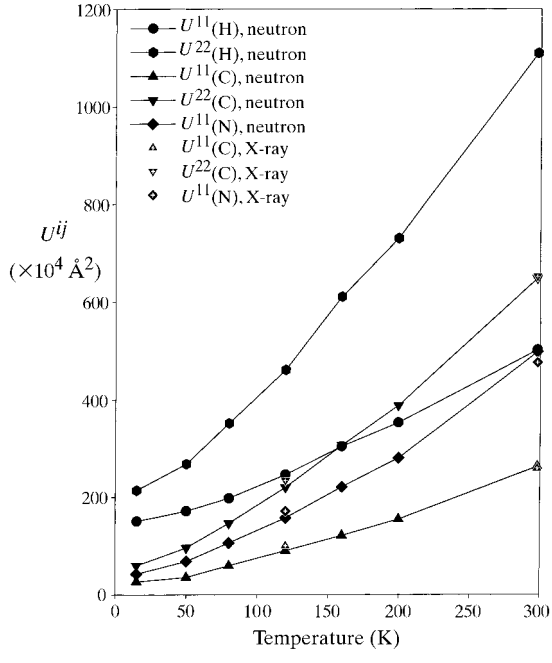

Figure 3
Unique diagonal values of **U**(H), **U**(C) and **U**(N) as a function of temperature (diffraction experiments by Duckworth *et al.*, 1970; Stevens & Hope, 1975; Kampermann *et al.*, 1994, 1995).

Table 2
Summary of results obtained with different models of motion for the analysis of ADP's of HMT from neutron diffraction data at six and nine temperatures (for explanation of symbols see text).

Values in square brackets refer to epsilon tensors restrained to the scaled *ab initio* values.

Model	*wR*2†	Gof n_{par}‡	ω_{lib} (cm^{-1})	$\gamma_{G(lib)}$	ω_{trans} (cm^{-1})	$\gamma_{G(trans)}$	ε(N) × 10^4 (Å^2)			ε(C) × 10^4 (Å^2)			ε(H) × 10^4 (Å^2)			ε(all) × 10^4 (Å^2)		
1_h	2.95	1.39	46.9 (2)	–	45.5 (2)	–	−11 (1)	–	–	−7 (1)	–	–	49 (1)	–	1 (1)			
								−8 (1)	–		−10 (1)	–		113 (1)	–			
		12							−8 (1)			−13 (1)			142 (1)			
1_at	2.10	0.991	46.7 (1)	–	52.7 (4)	5.3 (3)	−3 (1)	–	–	2 (1)	–	–	57 (1)	–	1 (1)			
								0 (1)	–		−2 (1)	–		120 (1)	–			
		3							0 (1)			−5 (1)			150 (1)			
1_al	1.79	0.851	52.7 (3)	4.5 (2)	45.5 (1)	–	−12 (1)	–	–	7 (1)	–	–	55 (1)	–	11 (1)			
								0 (1)	–		−1 (1)	–		133 (1)	–			
		3							0 (1)			−4 (1)			156 (1)			
1_atl	1.73	0.821	50.3 (2)	2.8 (2)	49.2 (2)	2.8 (2)	−7 (1)	–	–	−2 (1)	–	–	57 (1)	–	7 (1)			
								1 (1)	–		0 (1)	–		130 (1)	–			
		3							1 (1)			−3 (1)			155 (1)			
1_a	1.72	0.811	51.1 (3)	3.4 (2)	48.0 (4)	2.0 (3)	−9 (1)	–	–	−4 (1)	–	–	56 (1)	–	8 (1)			
								1 (1)	–		0 (1)	–		131 (1)	–			
		4							1 (1)			−3 (1)			156 (1)			
2_atl	3.84	1.80	51.1 (3)	4.7 (3)	56.6 (4)	4.7 (3)	[15]	–	–	[16]	–	–	68 (2)	–	5 (1)			
								[11]	–		[13]	–		138 (2)	–			
		7							[11]			[15]			165 (2)			
3_atl	3.23	1.52	52.3 (3)	4.0 (3)	51.5 (4)	4.0 (3)	−4 (1)	–	–	1 (1)	–	–	[68]	–	[7]			
								8 (1)	–		7 (1)	–		[136]	–			
		9							8 (1)			2 (1)			[188]			
4_atl	4.35	2.04	51.7 (4)	4.9 (3)	56.5 (5)	4.9 (3)	[15]	–	–	[16]	–	–	[68]	–	[7]			
								[11]	–		[13]	–		[136]	–			
		3							[11]			[15]			[188]			
5_atl	3.10	1.46	49.5 (3)	2.7 (3)	49.5 (4)	2.7 (3)	[15]	–	–	[16]	–	–	[68]	–	[7]	−16 (1)	–	–
								[11]	–		[13]	–		[136]	–			− 16 (1)	–
		4							[11]			[15]			[188]				−16 (1)
6_atl	2.39	1.13	49.0 (2)	2.5 (2)	49.6 (3)	2.5 (2)	[15]	–	–	[16]	–	–	72 (1)	–	3 (1)	−16 (1)	–	–
								[11]	–		[13]	–		139 (1)	–			−16 (1)	–
		8							[11]			[15]			167 (1)					−16 (1)
6_atl(9T)	3.13	1.53	49.0 (2)	2.3 (1)	48.0 (3)	2.3 (1)	[15]	–	–	[16]	–	–	65 (1)	–	4 (1)	−16 (1)	–	–
								[11]	–		[13]	–		136 (1)	–			−16 (1)	–
		8							[11]			[15]			165 (1)					−16 (1)

† $wR2 = [\sum w(U_{obs} - U_{calc})^2/\sum wU_{obs}^2]^{1/2} \times 100\%$. ‡ Gof = $[\sum w(U_{obs} \times U_{calc})^2/(n_{obs} - n_{par})]^{1/2}$; n_{par} = number of parameters; n_{obs} = number of observations = 54 [81 for 6_atl(9T)].

Table 3
Mean-square amplitudes from internal high-frequency vibrations for hydrogen.

For the coordinate system see text.

	T (K)	$\varepsilon_{11} \times 10^4$ (Å^2)	$\varepsilon_{22} \times 10^4$ (Å^2)	$\varepsilon_{33} \times 10^4$ (Å^2)	$\varepsilon_{13} \times 10^4$ (Å^2)
ADP analysis	15–298	65 (1)	136 (1)	165 (1)	4 (1)
Vibrational analysis from IR and Raman (Cyvin, 1972)	0	68	141	237	5
Ab initio calculations	15	68	136	188	7
Ab initio calculations	100	68	136	188	8
Inelastic neutron scattering (Thomas & Ghosh, 1975)	100	68	129	204	5
Ab initio calculations	298	71	140	214	13
Vibrational analysis from IR and Raman (Cyvin, 1972)	298	72	146	275	12

less negative and those of $\boldsymbol{\varepsilon}$(H) increase, but are still too small (Table 3). Agreement factors also improve, especially for the model with anharmonic libration (model 1_al). Separate Grüneisen parameters for libration and translation (Table 2, model 1_a) improve the agreement slightly, but the components of $\boldsymbol{\varepsilon}$(N) and $\boldsymbol{\varepsilon}$(C) are still negative or close to zero. In the final model, 1_atl, γ_G(lib.) and γ_G(trans.) were restrained to be equal; the refined value is close to the average of the two values in model 1_a and of the right order of magnitude (Grüneisen, 1926). Model 1_atl has one parameter less than model 1_a, gives about the same agreement factors, and is therefore more 'economic'. It has one more parameter than the harmonic one, but gives a substantially better description of the ADP's. For model 1_atl, the systematic discrepancies between observed and calculated U^{ij} found for the harmonic model are no longer present, the positive and negative differences being distributed more evenly (Fig. 4*b*). The increase in the differences with increasing temperature reflects a corresponding increase of $\sigma(U^{ij})$. Overall, the comparison of models 1_h and 1_atl documents the need for an anharmonic description of the ADP's of HMT measured between 15 and 200 K.

The $\boldsymbol{\varepsilon}$ tensors of N, C and H refined using model 1_atl are systematically smaller than those obtained from an *ab initio* vibrational analysis (see below), about 0.0016 Å^2 on average. Models with some or all $\boldsymbol{\varepsilon}$ tensors constrained to the calculated values give generally poor agreement factors, even worse than those of a simple harmonic model (Table 2, models 2_atl to 4_atl). Comparison between model 1_atl on one hand and 2_atl, 3_atl and 4_atl on the other indicates that the experimental ADP's are systematically too small. The discrepancy is therefore introduced into model 5_atl as a refinable parameter, the tensor $\boldsymbol{\varepsilon}$(all). If $\boldsymbol{\varepsilon}$(all) is assumed to reflect systematic error in the diffraction intensities, it is expected to show *m*3*m* Laue symmetry and thus to be isotropic. The *ad hoc* parameter $\boldsymbol{\varepsilon}$(all) improves the model significantly. The largest discrepancy between refined and calculated $\boldsymbol{\varepsilon}$ values is always found for ε_{33}(H). Thus, in the final model, 6_atl, $\boldsymbol{\varepsilon}$(H) is refined in addition to $\boldsymbol{\varepsilon}$(all).

The robustness of model 6_atl has been tested by refining it against all nine sets of diffraction data (Duckworth *et al.*, 1970; Stevens & Hope, 1975; Kampermann *et al.*, 1994, 1995). The introduction of three additional sets of data in the analysis and the consequent extension of the temperature range do not lead to significant changes in the model of motion [Table 2, model 6_atl(9*T*)].

The agreement factors of model 6_atl are better than those of the harmonic model 1_h. They are inferior to those of the family of anharmonic models 1_a but the number of refinable parameters is smaller in model 6_atl than in models 1. The highest correlation coefficient in model 6_atl is between $\omega_{\rm lib}$ and γ_G (0.87). Other correlation coefficients larger than 0.5 are between $\omega_{\rm trans}$ and γ_G (0.77), $\omega_{\rm trans}$ and $\varepsilon_{\rm all}$ (0.75), and $\omega_{\rm trans}$ and $\omega_{\rm lib}$ (0.62). Together with the small standard uncertainties of the parameters, they indicate that the model is well determined. As will be discussed below, all its numerical results are physically reasonable and compare well with numbers obtained from independent experiments. We therefore consider model 6_atl as the best partition of the observed ADP's into temperature-dependent contributions from low-frequency vibrations, temperature-independent contributions from high-frequency vibrations and contributions from inadequate treatment of absorption, extinction, valence electron density *etc.*

5. Intramolecular vibrations of hexamethylenetetramine

The temperature-independent contributions to the ADP's coming from intramolecular vibrations have been calculated by *ab initio* methods for comparison with the corresponding values from the ADP analysis. The calculations have been performed at the restricted Hartree–Fock (RHF) level using *GAMESS* (Schmidt *et al.*, 1993). The structure was optimized and analytical second derivatives of the potential energy calculated, both at the 6-311G** basis-set level. Throughout all calculations, T_d molecular symmetry was enforced. The starting point for the geometry optimization was the 15 K neutron structure (Kampermann *et al.*, 1995). The optimized (or equilibrium) geometry is given in Table 1, where it is compared to the 15 K neutron geometry.

As expected for this level of theory, the calculated equilibrium distances are a little shorter than the experimental values (not corrected for librational shortening or for lengthening due to anharmonic bond-stretching potentials). The calculated angles also differ somewhat from experiment,

especially the ones including hydrogen atoms. The harmonic vibrational frequencies and IR intensities have been calculated from the elements of the force-constant matrix using masses of 12, 1.00782 and 14.0307 a.m.u. for C, H and N, respectively.

A molecule of HMT in a crystal has 66 degrees of vibrational freedom: six correspond to external modes of vibration, namely three translations and three librations which the molecule undergoes as a rigid body; the other 60 correspond to internal vibrations. The *ab initio* frequencies of the internal normal modes have values in the range 402 to 3247 cm^{-1}, after scaling with a factor of 0.91 to match the observed frequencies (Bertie & Solinas, 1974). The normal-mode mean-square displacements were calculated for each scaled frequency with equation (1). Atomic displacements were obtained from equation (5). Results are given in Table 3.

The 60 scaled frequencies corresponding to internal vibrations and the six frequencies corresponding to external normal modes have been used to calculate the vibrational contribution to the specific heat ($\bar{C}_V$), according to the relation (Andrews, 1963)

$$\bar{C}_V = \sum_j mNk(\Theta_{E_j}/T)^2 \frac{\exp(\Theta_{E_j}/T)}{[\exp(\Theta_{E_j}/T)-1]^2}, \qquad (22)$$

where the sum runs over the unique normal modes j; m is their degeneracy, N is Avogadro's number, k is the Boltzmann constant, T is the absolute temperature; $\Theta_{E_j} = \hbar\omega_{\rm eff}(j)/k = 1.437\tilde{\nu}_{\rm eff}(j)$, where Θ_{E_j} is the Einstein temperature in K and $\tilde{\nu}$ the wave number in cm^{-1}.

6. Discussion

The libration frequency ω_0 refined from ADP's varies according to the model of motion in the range 46.7 (1)–52.7 (3) cm^{-1}; the translation frequency shows a slightly wider range, 45.5 (3)–56.6 (4) cm^{-1}. These values can be compared to the frequency distribution functions for intermolecular modes computed by Dolling & Powell (1970) with a force field derived from coherent neutron inelastic scattering measurements on DHMT at 100 and 298 K. The density of states for translation extends between 0 and 75 cm^{-1} with maxima at 51 and 69 cm^{-1}, the corresponding function for libration extends from 35 to 63 cm^{-1} with maxima between 35 and 41 cm^{-1} and between 50 and 55 cm^{-1}. They reflect the dispersion of the acoustic and optic branches, respectively, and show that there is a wide range of frequencies where the total density of states receives contributions from both translation and libration. In the mean-field model, the density of states for HMT is approximated with two δ functions, one for translation and the other for libration. The frequencies of the various models reported in Table 2 all fall within the distribution functions calculated by Dolling & Powell (1970). The value of $\omega_{\rm eff}$(lib) for HMT is 44.3 cm^{-1} at 298 K (model 6_atl), to be compared with the expectation value $\langle 1/\omega^2\rangle^{-1/2}$ of 44.6 cm^{-1}, calculated by Dolling & Powell (1970) for HMT on the basis of their measurements at room temperature on DHMT.

The Grüneisen parameters obtained by ADP analyses vary in the range 2.3 (1)–5.3 (3). The higher value occurs when anharmonic corrections are applied to translation only. These values may be compared to the temperature dependence of the dispersion curves observed by Dolling & Powell (1970) at 100 and 298 K. Grüneisen constants have been estimated at

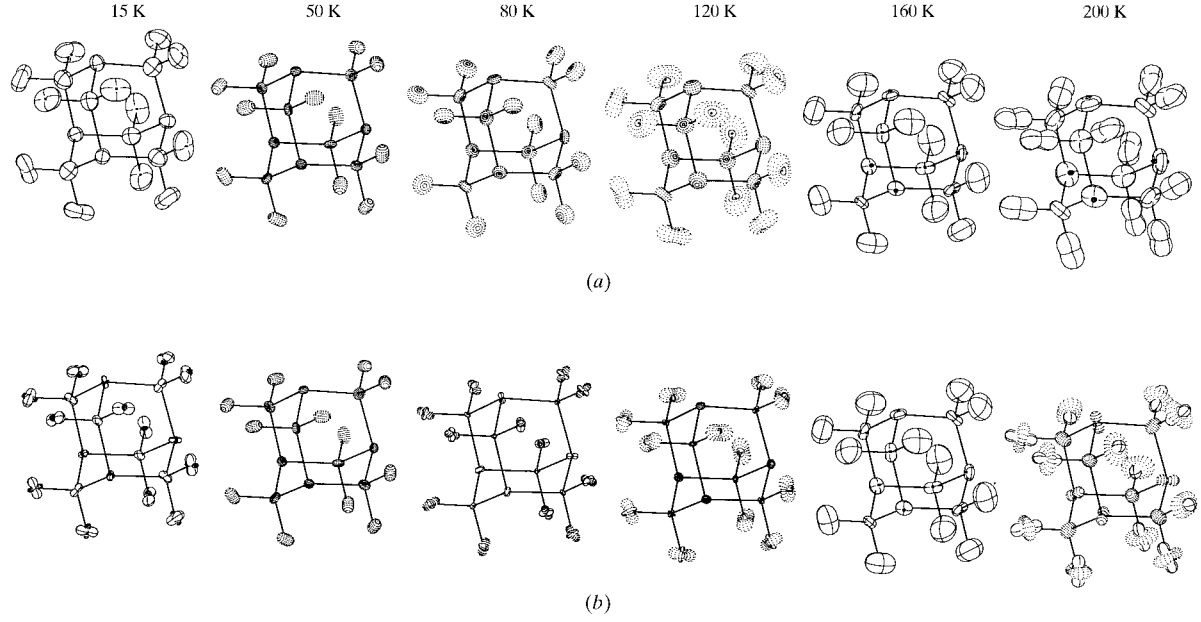

Figure 4
Difference displacement parameters ($\mathbf{U}_{\rm obs} - \mathbf{U}_{\rm calc}$) for HMT at 15, 50, 80, 120, 160, 200 K, displayed as root-mean-square surfaces (Hummel *et al.*, 1990); solid lines indicate positive differences, dotted lines indicate negative differences, scale factor 9.23: (*a*) model 1_h, (*b*) model 1_atl. Note that the differences for the hydrogen atoms are bigger than for carbon and nitrogen atoms because $\sigma(U^{ij})$ for the hydrogen atoms are a factor about 2 to 5 times bigger than those of carbon and nitrogen atoms. The differences increase with temperature because $\sigma(U^{ij})$ increases with temperature.

Table 4
Calculated mean-square amplitudes from internal high-frequency vibrations for nitrogen and carbon.

For the coordinate system, see text.

	T (K)	ε_{11}(N) ($\times 10^4$Å^2)	ε_{22}(N) ($\times 10^4$Å^2)	ε_{11}(C) ($\times 10^4$Å^2)	ε_{22}(C) ($\times 10^4$Å^2)	ε_{33}(C) ($\times 10^4$Å^2)
Vibrational analysis from IR and Raman (Cyvin, 1972)	0	13	10	15	12	16
Ab initio calculations	15	15	11	16	13	15
Vibrational analysis from IR and Raman (Cyvin, 1972)	298	15	12	16	15	19
Ab initio calculations	298	16	12	17	15	18

each point in the Brillouin zone for which a frequency has been measured at both 100 and 298 K. The values obtained along the directions ($\zeta\zeta\zeta$) and (00ζ) using the expression

$$\gamma_G = -[(\omega_{298} - \omega_{100})/\omega_{100}][V_{100}/(V_{298} - V_{100})] \qquad (23)$$

have been averaged; they are, respectively, 2.2 and 2.5, in good agreement with the values refined using model 6_atl with data from either six or nine temperatures.

In Table 3, the values for $\boldsymbol{\varepsilon}$(H) refined in model 6_atl are compared to: (i) those calculated with the *ab initio* data at 15, 100 and 298 K; (ii) those determined by Thomas & Ghosh (1975) from a normal-coordinate analysis based on neutron inelastic scattering data at 100 K; and (iii) those obtained by Cyvin (1972) from a vibrational analysis at 298 K based on IR and Raman data. By definition, values of $\boldsymbol{\varepsilon}$ refined from ADP's are independent of temperature. The *ab initio* values in Table 3 show that this is a good approximation except for ε_{33}(H), which increases by ~0.0025 Å^2 (or 14%) between 0 and 298 K. This increase is small compared to that of the ADP's (Fig. 3). The values of ε_{11} and ε_{22} vary little, while the values of ε_{33} vary substantially with the method of determination. The component ε_{33}(H) from ADP analysis is ~10–20% lower than the *ab initio* values. Comparable differences have also been observed for $OC(NH_2)_2$, C_6D_6 (Förtsch, 1997; Capelli *et al.*, 2000) and C_6H_6 in the C_6H_6–$AgClO_4$ complex (Capelli, 1999). The IR and Raman data are ~30% larger than *ab initio* values. The result from neutron inelastic scattering is ~10% higher than the *ab initio* value. The discrepancies between *ab initio* and spectroscopic results are probably due to a combination of experimental and assignment errors in the spectroscopic data and deficiencies in the *ab initio* calculations not accounted for by the frequency scaling. In Table 4, the values for $\boldsymbol{\varepsilon}$(N) and $\boldsymbol{\varepsilon}$(C) calculated *ab initio* and used in the refinement are compared to those reported by Cyvin at 0 and 298 K (Cyvin, 1972). They agree well even though corresponding values for $\boldsymbol{\varepsilon}$(H) show some significant differences (Table 3).

It should be remembered here that the results discussed above have been obtained including in the model of motion an *ad hoc* overall tensor $\boldsymbol{\varepsilon}$(all) that cannot be interpreted in terms of motion. This tensor refines to the same magnitude in three different models [Table 2, models 5_atl, 6_atl and 6_atl(9*T*)]. Its negative value implies that the observed ADP's are systematically smaller than those corresponding to the models of motion. What is $\boldsymbol{\varepsilon}$(all) due to? Kampermann *et al.* (1995) have reported that their neutron data are severely affected by extinction and have corrected for this using three different models. No extinction correction was applied to the 120 K X-ray data (Kampermann *et al.*, 1994) and only one reflection severely affected by extinction was left out of the refinement of the 298 K X-ray data (Stevens & Hope, 1975). We believe that the systematic discrepancy parameterized by $\boldsymbol{\varepsilon}$(all) is related to effects of extinction that have been insufficiently accounted for. This would indeed give ADP's that are too small. If true, this conclusion underlines the observation by Kampermann *et al.* (1995) that none of the presently available theories treat severe extinction adequately.

Finally, the molar heat capacity $\bar{C}_V$ calculated from the translational and librational frequencies of model 6_atl and from the scaled internal *ab initio* frequencies are compared graphically in Fig. 5 with the experimental values of $\bar{C}_P$ measured by Chang & Westrum (1960). The overall agreement between experimental and calculated curves is surprisingly good. In the temperature range 15–80 K, calculated values are higher than experimental ones. This is due to the Einstein approximation used in the ADP analysis (Bürgi & Capelli, 2000), which neglects the linear dependence of the acoustic phonons on the wavevector in the inner part of the Brillouin zone. In the temperature range 120–350 K, the calculated curve is lower than the experimental one. There are two likely reasons for this discrepancy: (i) frequencies for the internal

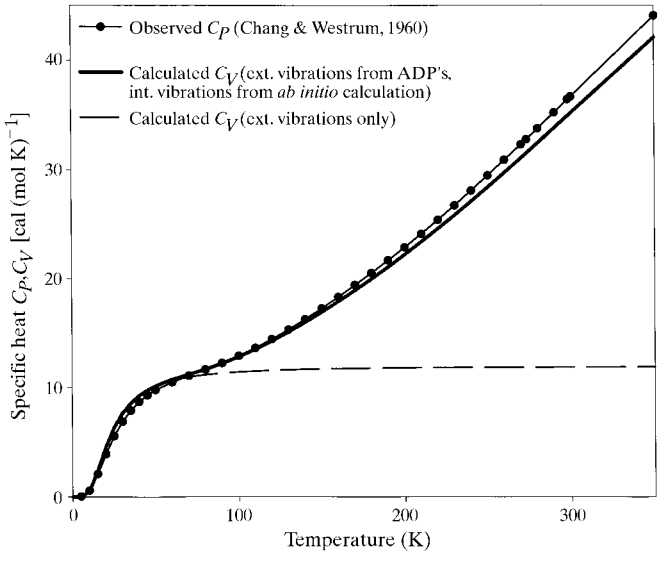

Figure 5
Molar heat capacity of HMT: $\bar{C}_V$ calculated compared to $\bar{C}_P$ measured by Chang & Westrum (1960).

modes of vibration are too large, implying that the factor used for scaling the *ab initio* frequencies is too large, or (ii) the anharmonic contribution to $\bar{C}_P$ becomes important. If only the first possibility is invoked, the scale factor would have to be 0.875 instead of 0.91. Such a small value seems unlikely if compared to literature data (Scott & Radom, 1996). If the second possibility is invoked, the required anharmonic contribution is $\Delta C_P = \bar{C}_P - \bar{C}_V = V\chi^2 T/\kappa_0$, with V the molar volume, χ the volume expansion coefficient and κ_0 the compressibility of the crystal at zero pressure. Using this relation, we estimated κ_0 from the difference between the two curves in the temperature range 200–350 K. The calculated average value of the compressibility is 0.231 GPa^{-1}, corresponding to a bulk modulus of 4.33 GPa.

Bridgman (1947) performed volumetric measurements of HMT in the pressure range 0–3.92 GPa. The compressibility κ_0 was obtained by fitting his data to the Vinet universal equation of state (Vinet *et al.*, 1986, 1989).[1] The compressibility is found to be 0.116 (5) GPa^{-1}, corresponding to a bulk modulus of 8.96 (37) GPa. The bulk modulus calculated from elastic constants is 8.36 GPa (Haussühl, 1958). These experimental values indicate that our simple-minded estimate of the compressibility is too large, that the actual difference $\bar{C}_P - \bar{C}_V$ is about twice as large, and that the scaling factor should be 0.95. Compared to literature data, this value seems too high (Scott & Radom, 1996). Whether this is due to the use of an isolated molecule model in the *ab initio* calculation or to a systematic error in $\bar{C}_P$ cannot be decided on the basis of the information presently available.

7. Conclusions

Anharmonic corrections have been introduced into a molecular-mean-field harmonic normal-mode model of the temperature evolution of ADP's. Changes of frequency with temperature are taken into account by a Grüneisen parameter for each normal mode. The normal vibrations are assumed not to change their shape during thermal expansion. Such a description has the same algebraic form as a harmonic model and is therefore called quasi-harmonic.

The model has been used to analyze ADP's of HMT obtained from neutron and X-ray diffraction experiments in the temperature range 15–298 K. The analysis allows, for the first time, dissection of ADP's into contributions from low-frequency high-amplitude vibrations and their anharmonicity, from high-frequency low-amplitude vibrations, and from other temperature-independent effects such as inadequate treatment of absorption, extinction, valence-electron density *etc.* The librational and translational frequencies and the Grüneisen parameters obtained from ADP's are comparable in magnitude to those calculated from dispersion curves pertaining to temperatures of 100 and 298 K (Dolling & Powell, 1970). If the model for calculating the ADP's includes an *ad hoc* additive term to account for insufficient extinction corrections of the diffraction data, then the temperature-independent part of the ADP's due to high-frequency internal vibrations compares reasonably well with results from *ab initio* calculations on HMT in the gas phase. Finally, the heat capacity $\bar{C}_V$ of HMT has been calculated, the contribution of the compressibility to $\bar{C}_P$ has been estimated and the results compared to experimental data.

[1] The Vinet universal equation of state is $P = [3B_0(1-X)/X^2] \times \exp[1.5(B_0' - 1)(1-X)]$, where $X = (V/V_0)^{1/3}$ and V_0 is the volume at zero pressure. B_0 and B_0' are, respectively, the isothermal bulk modulus and its first pressure derivative both at zero pressure.

References

Andrews, F. C. (1963). *Equilibrium Statistical Mechanics.* New York: Wiley.

Becka, L. N. & Cruickshank, D. W. J. (1963). *Proc. R. Soc. London Ser. A*, **273**, 435–454.

Bertie, J. E. & Solinas, M. (1974). *J. Chem. Phys.* **61**, 1666–1677.

Birkedal, H., Bürgi, H. B., Capelli, S. C. & Schwarzenbach, D. (1997). ECM-17, Poster abstract P2.7-3, Lisboa, Portugal.

Bridgman, P. W. (1947). *Proc. Am. Acad. Arts Sci.* **76**, 71–87.

Brüesch, P. (1982). *Phonons: Theory and Experiments I, Lattice Dynamics and Models of Interatomic Forces. Springer Series in Solid State Sciences*, Vol. 34. Berlin/Heidelberg/New York: Springer-Verlag.

Buckingham, R. A. (1938). *Proc. R. Soc. London Ser. A*, **168**, 264–283.

Bürgi, H. B. (1995). *Acta Cryst.* B**51**, 571–579.

Bürgi, H. B. & Capelli, S. C. (2000). *Acta Cryst.* A**56**, 403–412.

Bürgi, H. B. & Förtsch, M. (1999). *J. Mol. Struct.* **485–486**, 457–463.

Capelli, S. C. (1999). PhD thesis, University of Bern, Switzerland.

Capelli, S. C., Förtsch, M. & Bürgi, H. B. (2000). *Acta Cryst.* A**56**, 413–424.

Chang, S.-S. & Westrum, E. F. (1960). *J. Phys. Chem.* **64**, 1547–1551.

Coppens, P. (1993). *International Tables for Crystallography*, Vol. B, edited by U. Shmueli, pp. 10–22. Dordrecht: Kluwer Academic Publishers.

Coppens, P. (1997). *X-ray Charge Density and Chemical Bonding.* New York: Oxford University Press.

Cyvin, S. J. (1968). *Molecular Vibrations and Mean Square Amplitudes.* Amsterdam: Elsevier.

Cyvin, S. J. (1972). *Molecular Structures and Vibrations.* Amsterdam: Elsevier.

Dickinson, R. G. & Raymond, A. L. (1923). *J. Am. Chem. Soc.* **45**, 22–29.

Dolling, G. & Powell, B. M. (1970). *Proc. R. Soc. London Ser. A*, **319**, 209–235.

Duckworth, J. A., Willis, B. T. M. & Pawley, G. S. (1970). *Acta Cryst.* A**26**, 263–271.

Evans, J. S. O., Mary, T. A. & Sleight, A. W. (1997). *Physica (Utrecht) B*, **241**, 311–316.

Förtsch, M. (1997). PhD thesis, University of Bern, Switzerland.

Grüneisen, E. (1926). *Handbuch der Physik*, edited by H. Geiger & K. Scheel, Vol. 10, pp. 1–59. Berlin: Springer.

Haussühl, S. (1958). *Acta Cryst.* **11**, 58–59.

Higgs, P. W. (1955). *Acta Cryst.* **8**, 99–104.

Hummel, W., Hauser, J. & Bürgi, H. B. (1990). *J. Mol. Graphics*, **8**, 214–220.

Johnson, C. K. & Levy, H. A. (1974). *International Tables for X-ray Crystallography*, Vol. IV, pp. 314–319. Birmingham: Kynoch Press. (Present distributor: Kluwer Academic Publishers, Dordrecht.)

Kampermann, S. P., Ruble, J. R. & Craven, B. M. (1994). *Acta Cryst.* B**50**, 737–741.

Kampermann, S. P., Sabine, T. M. & Craven, B. M. (1995). *Acta Cryst.* A**51**, 489–497.

Lennard-Jones, J. E. (1924). *Proc. R. Soc. London Ser. A*, **106**, 441–462, 463–477.

Morse, P. M. (1929). *Phys. Rev*. **34**, 57–64.
Schmidt, M. W., Baldridge, K. K., Boatz, J. A., Elbert, S. T., Gordon, M. S., Jensen, J. H., Koseki, S., Matsunaga, N., Nguyen, K. A., Su, S., Windus, T. L., Dupuis, M. & Montgomery, J. A. (1993). *J. Comput. Chem.* **14**, 1347–1363.
Scott, A. P. & Radom, L. (1996). *J. Phys. Chem.* **100**, 16502–16513.
Stevens, E. D. & Hope, H. (1975). *Acta Cryst.* A**31**, 494–498.
Stewart, R. F. (1976). *Acta Cryst.* A**32**, 565–574.
Terpstra, M., Craven, B. M. & Stewart, R. F. (1995). *Acta Cryst.* A**49**, 685–692.
Thomas, H. (1971). *Structural Phase Transitions and Soft Modes*, edited by E. J. Samuelson, E. Andersen & J. Feder, pp. 15–41. Oslo: Universitetsforlaget.
Thomas, M. W. & Ghosh, R. E. (1975). *Mol. Phys.* **29**, 1489–1506.
Vinet, P., Ferrante, J., Smith, J. R. & Rose, J. H. (1986). *J. Phys. C*, **19.** L467–L473.
Vinet, P., Rose, J. H., Ferrante, J. & Smith, J. R. (1989). *J. Phys. Condens. Matter*, **1**, 1941–1963.
Willis, B. T. M. & Pryor, A. W. (1975). *Thermal Vibrations in Crystallography*. Cambridge University Press.